J|A|C|S ARTICLES

Published on Web 06/28/2010

In Situ EPR Study of Chemical Reactions in Q-Band at Higher Temperatures: A Challenge for Elucidating Structure−Reactivity Relationships in Catalysis

Reinhard Stösser,[‡] Ulrich Marx,[†] Werner Herrmann,[§] Jabor K. Jabor,[†] and Angelika Brückner*[,†]

Leibniz-Institut für Katalyse e. V. an der Universität Rostock, Albert-Einstein-Strasse 29a, D-18059 Rostock, Germany, Institute of Chemistry, Humboldt University of Berlin, Brook-Taylor-Strasse 2, D-12489 Berlin, Germany, and Institute of Pharmacy, Free University of Berlin, Kelchstrasse 31, D-12169 Berlin, Germany

Received April 26, 2010; E-mail: angelika.brueckner@catalysis.de

Abstract: For the first time, heterogeneous catalytic reactions have been monitored by in situ EPR spectroscopy in the Q-band using a homemade heatable probe head equipped with a flow reactor. The reactions of Al_2O_3-supported TEMPO with NO and H_2 as well as of SiO_2/Al_2O_3-supported $H_4PVMo_{11}O_{40}$ with methanol and formaldehyde were studied up to 400 °C. TEMPO radicals are immobilized on the support in positions which impose a different reactivity to NO and H_2. This may be due to different accessibility, which changes during thermal treatment. By combined evaluation of anisotropic X- and Q-band spectra with a complex hyperfine structure (e.g., from VO^{2+}), spin Hamiltonian parameters can be derived with higher precision, since limits of the specific resolution in both frequency bands are compensated for. In addition to VO^{2+}, Mo^{5+} is formed above 180 °C depending on the O_2 content of the feed, which is easily discriminated in the Q-band but not in the X-band.

1. Introduction

In situ investigation of catalysts under real reaction conditions by suitable spectroscopic methods is a rapidly growing research field, since it is the most authentic and reliable way to obtain information on structure−reactivity relationships which are inevitable for a knowledge-based catalyst design beyond trial and error. Among the variety of sophisticated techniques, Electron Paramagnetic Resonance (EPR) has experienced a rapid development as a tool for monitoring solid catalysts under reaction conditions during the past two decades. This is reflected in several reviews.[1−5] Besides a few studies on the behavior of radicals in catalytic reactions,[6,7] the majority of in situ EPR studies in catalysis deals with heterogeneous gas phase reactions using highly dispersed supported transition metal ions as active sites, among them CrO_x species in the aromatization and dehydrogenation of alkanes,[8] supported VO_x species during oxidation of SO_2 and oxidative dehydrogenation of propane,[9] supported MoO_x species in selective oxidation of propane and methanol,[10] and Fe and Cu ions within zeolites in selective catalytic reduction of NO.[11,12] However, it has also been shown that changes of spin−spin exchange interactions evident in unsupported vanadium phosphates with closely neighboring VO_x sites can beneficially be explored by in situ EPR to derive information on the behavior of the unsupported mixed metal oxides during reaction.[13]

All of the above-mentioned studies were performed in the X-band at a microwave frequency of ∼9.5 GHz. However, particularly for systems which contain different paramagnetic species and give rise to complex spectra with several superimposed signals, it might be very helpful to record EPR spectra at a higher magnetic field in the Q-band ($\nu \approx 35$ GHz), since this provides higher spectral resolution and higher sensitivity. Furthermore, EPR spectra which are characterized by spin exchange and/or motional effects can differ markedly in the X- and Q-band, since the visibility of such effects depends on the difference between the microwave frequency and the rate of spin exchange and/or molecular motion. Performing in situ experiments in the Q-band is a true experimental challenge for several reasons: On the one hand, no commercial equipment is available for Q-band EPR studies at elevated temperatures which are needed for most heterogeneous catalytic gas phase reactions. On the other hand, a heatable quartz plug-flow microreactor

[†] Leibniz-Institut für Katalyse e. V. an der Universität Rostock.
[‡] Humboldt University of Berlin.
[§] Free University of Berlin.

(1) Brückner, A. *Adv. Catal.* **2007**, *51*, 265–308.
(2) Brückner, A. In *In situ Spectroscopy of Catalysts*; Weckhuysen, B. M., Ed.; American Scientific Publishers: Stevenson Ranch, CA, 2004; pp 219−251.
(3) Labanowska, M. *ChemPhysChem* **2001**, *2*, 712–731.
(4) Dyrek, K.; Che, M. *Chem. Rev.* **1997**, *97*, 305–331.
(5) Sojka, Z. *Catal. Rev. Sci. Eng.* **1995**, *37*, 462–512.
(6) Horikoshi, S.; Hidaka, H.; Serpone, N. *Chem. Phys. Lett.* **2003**, *376*, 475–480.
(7) Lunsford, H. J. *Catal. Today* **1990**, *6*, 235–259.
(8) Brückner, A. *Chem. Commun.* **2001**, 2122–2123.
(9) Eriksen, K. M.; Fehrmann, R.; Bjerrum, N. J. *J. Catal.* **1991**, *132*, 263–265.
(10) Sojka, Z.; Che, M. *J. Phys. Chem.* **1995**, *99*, 5418–5430.
(11) Santhosh Kumar, M.; Schwidder, M.; Grünert, W.; Bentrup, U.; Brückner, A. *J. Catal.* **2006**, *239*, 273–286.
(12) Kucherov, A. V.; Gerlock, J. L.; Jen, H.-W.; Shelef, M. *J. Phys. Chem.* **1994**, *98*, 4892–4894.
(13) Brückner, A. *Top. Catal.* **2006**, *38*, 133–139.

must be placed into the Q-band cavity. The inner dimensions of the EPR cavity must be tuned to the wavelength of the microwave radiation, which is 31 mm in the X-band but only 8 mm in the Q-band. This means that the outer diameter of the dewar mantle surrounding the Q-band plug-flow reactor should not be larger than 5.5 mm and the reactor tube itself should be smaller than 2 mm in diameter while still enabling reactant gases to flow through the catalyst bed (see also Experimental Section). Moreover, broad-band tuning of the small Q-band cavity including heating dewar and microreactor tube to the microwave bridge without considerable loss of the quality factor is a technical challenge.

In this work, we developed the first homemade probe head for in situ EPR studies of heterogeneous catalytic reactions in the Q-band up to temperatures of 500 °C. The potential of this novel setup has been tested for two systems: (i) the reaction of an alumina-supported radical species, namely 2,2,6,6-tetramethylpiperidine-1-oxyl (TEMPO), with NO and (ii) the reaction of the heteropoly acid $H_4PVMo_{11}O_{40}\cdot xH_2O$ (HPVMo) supported on silica−alumina with methanol (MeOH) and formaldehyde (FA). These compounds have been chosen since they both contain paramagnetic entities, being thus suitable systems for EPR studies, and are meaningful as oxidizing agents (TEMPO[14−16]) or catalysts (HPVMo) for selective catalytic oxidation reactions, e.g. of alcohols. In particular, vanadium-containing polyoxometallates with a Keggin-type structure, such as those containing $[PVMo_{11}O_{40}]^{4-}$ anions, revealed themselves to be suitable catalysts for the selective oxidation of hydrocarbons and alcohols, e.g. of methanol and ethanol,[17,18] of methacrolein (MAC) to methacrylic acid (MAA),[19,20] and of isobutane to MAC and MAA,[21−23] and for the oxidative dehydrogenation of isobutyric acid to MAA.[24−26] By using pulsed electron nuclear double resonance (ENDOR) in the X- and Q-band, it has been found that the catalytically relevant VO^{2+} species are directly attached to the outer surface of the $[PVMo_{11}O_{40}]^{4-}$ by four V−O−Mo bidges.[27] However, although such sophisticated magnetic resonance methods can provide much more detailed structural information than conventional continuous wave (cw) EPR investigations, they cannot be used for monitoring polyoxometallates during catalytic reactions, since they require very low (usually liquid helium) temperatures for spectra recording.

For some of the above-mentioned reactions, in situ cw-EPR studies in the X-band have been performed.[17,23,24] However, the interpretation of the spectra revealed to be not straightforward, due to the superposition of signals from several V^{4+} and/or Mo^{5+} species. It can be expected that these difficulties can at least partially be overcome by in situ EPR measurements in the Q-band due to the higher resolution and sensitivity. In this work, the wider insight, gained particularly from the combined evaluation of X- and Q-band studies on the same catalytic system under similar reaction conditions, is explicitly demonstrated for the first time. However, although the examples in this work have been chosen with respect to their importance in heterogeneous catalysis, it must be emphasized that the application of the new Q-band setup is not restricted to this area but can be used for the study of other suitable paramagnetic species as well, e.g. in surface or solid state chemistry.

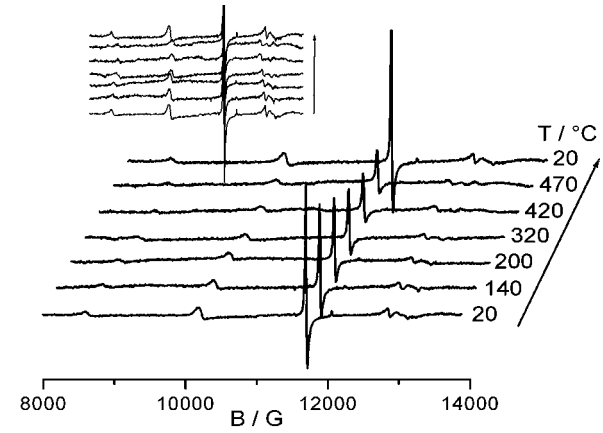

Figure 1. Q-band EPR spectra of α-Al_2O_3: Fe^{3+} at different temperature. Arrow denotes sequence of heating/cooling. The inset shows the temperature-dependent shift of the fine structure signals.

2. Results and Discussion

2.1. Test of the Q-Band Setup at Elevated Temperature. To check the proper function of the setup, we selected a sample of α-Al_2O_3 doped with less than 0.01 mol % Fe^{3+}, which had been well characterized previously by experimental and calculated EPR spectra at room temperature and different microwave frequencies, including the X- and Q-band.[28] The Fe^{3+} ions are incorporated in Al^{3+} lattice positions, which impose a distortion of their local coordination sphere. The EPR signals at room temperature (Figure 1) arise from the fine structure of the five unpaired electrons ($S = 5/2$) and can be reproduced by spectra simulation with the parameters $g = 2.003$, $b_2^0 = 1705 \times 10^{-4}$ cm^{-1}, $b_4^0 = -108 \times 10^{-4}$ cm^{-1}, $b_4^3 = 2181 \times 10^{-4}$ cm^{-1}, and $b_2^2 = 0$, in good agreement with previous measurements in Q-band at room temperature.[28] Stepwise heating to 470 °C changes the local symmetry of the Fe^{3+} coordination sphere due to the anisotropy of the thermal extension of the unit cell of α-Al_2O_3 (Figure 1). The zero-field splitting (zfs) is reduced, and the widths of the fine structure signals are enlarged at elevated temperatures, due to thermally induced averaging processes, which cause a statistically larger distribution of the zfs parameters, particularly that of b_2^2.[28] All spectral changes are completely reversible on cooling to room temperature. The Q-band spectrum of the sample at 20 °C measured after cooling from 470 °C shows identical signal positions and, thus, can be described by the same zfs parameters before heating. This shows

(14) Jiang, N.; Ragauskas, A. J. *J. Org. Chem.* **2006**, *71*, 7087–7090.
(15) Braqd, P. L.; Besemer, A. C.; Bekkum, H. V. *J. Mol. Catal. A: Chem.* **2001**, *170*, 35–42.
(16) Gilhespy, M.; Lok, M.; Baucherel, X. *Chem. Commun.* **2005**, 1085–1086.
(17) Lee, J. K.; Russo, V.; Melsheimer, J.; Köhler, K.; Schlögl, R. *Phys. Chem. Chem. Phys.* **2000**, *2*, 2977–2983.
(18) Popa, A.; Sasca, V.; Halasz, J. *Appl. Surf. Sci.* **2008**, *255*, 1830–1835.
(19) Mizuno, N.; Misono, M. *Chem. Rev.* **1998**, *98*, 199–217.
(20) Marosi, L.; Otero Areán, C. *J. Catal.* **2003**, *213*, 235–240.
(21) Cavani, F.; Mezzogori, R.; Pigamo, A.; Trifirò, F.; Etienne, E. *Catal. Today* **2001**, *71*, 97–110.
(22) Sultan, M.; Paul, S.; Fournier, M.; Vanhove, D. *Appl. Catal., A* **2004**, *259*, 141–152.
(23) Brückner, A.; Scholz, G.; Heidemann, D.; Schneider, M.; Herein, D.; Bentrup, U.; Kant, M. *J. Catal.* **2007**, *245*, 369–380.
(24) Aboukais, A.; Haubtmann, C.; André, C. C.; Desquilles, C.; Dourdin, M.; Mathes-Juventin-Andrieu, I.; Aissi, F. C.; Guelton, M. *J. Chem. Soc., Faraday Trans.* **1995**, *91*, 1025–1029.
(25) Ilkenhans, Th.; Herzog, B.; Braun, Th.; Schlögl, R. *J. Catal.* **1995**, *153*, 275–292.
(26) Marchal-Roch, C.; Bayer, R.; Moisan, J. F.; Tézé, A.; Hervé, G. *Top. Catal.* **1996**, *3*, 407–419.
(27) Gutjahr, M.; Hoentsch, J.; Böttcher, R.; Storcheva, O.; Köhler, K.; Pöppl, A. *J. Am. Chem. Soc.* **2004**, *126*, 2905–2911.
(28) Buzaré, J. Y.; Silly, G.; Klein, J.; Scholz, G.; Stösser, R.; Nofz, M. *J. Phys.: Condens. Matter* **2002**, *14*, 10331–10348.

Scheme 1. Structure of the 2,2,6,6-Tetramethylpiperidine-1-oxyl (TEMPO) Radical

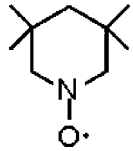

that the new Q-band setup is working properly up to a temperature of 470 °C.

2.2. Thermal Behavior and Reactions of Supported TEMPO Radicals. Alumina is a well-known support for creating highly dispersed catalytically active species on its surface, which can be used as solid catalysts in heterogeneous catalytic gas phase reactions. These comprise a wide variety of transition metal ions, either supported as oxidic species[29,30] or as immobilized organometallic complexes.[31,32] There are numerous procedures known which can be used to deposit catalytically active species on support surfaces. In this work, we have dispersed the TEMPO radical (Scheme 1), known to act as an organocatalyst in alcohol oxidations, on the support surface by milling α-Al_2O_3 or AlOOH together with TEMPO.

In highly diluted solutions, in which the rotational motion of the TEMPO molecule is not hindered by mutual interactions with each other or with the solvent molecules, the EPR spectrum of TEMPO should consist of an isotropic signal which is split into three equally intense hyperfine structure (hfs) lines, separated by the hyperfine coupling constant *A*, which arise from the interaction of the unpaired electron spin with the nuclear spin of the ^{14}N nucleus ($I = 1$).[33] As can be seen from Figure 2, this is not true for TEMPO attached to the surface of α-Al_2O_3. The three hfs lines can still be seen, but the spectrum as a whole is strongly anisotropic since the molecular motion of the TEMPO molecules is strongly hindered by their immobilization on the alumina surface. This is particularly evident at room temperature before heating and does not change much up to 180 °C (Figure 2). At 230 °C a marked line narrowing is evident which suggests a less restricted molecular rotation at higher temperatures. Interestingly, this process already takes place in a temperature range which is important for many catalytic reactions. After cooling and storing the sample for 18 h at room temperature, the EPR spectrum consists of a superposition of two signals with different line widths.

It has been shown previously for homogeneous TEMPO solutions in different ionic liquids that the motional behavior of the TEMPO molecules can be characterized by the rotational

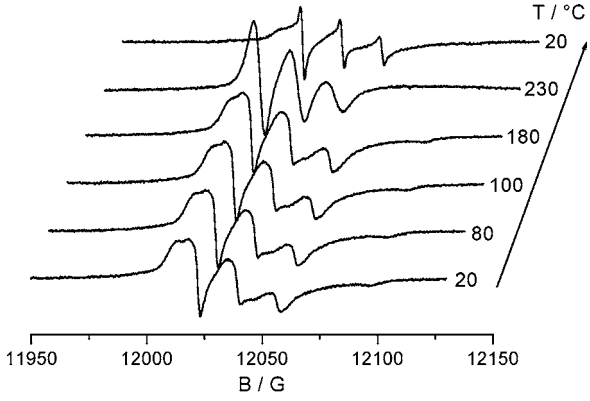

Figure 2. EPR spectra of TEMPO/α-Al_2O_3 recorded in Q-band as a function of temperature. Arrow denotes sequence of heating/cooling.

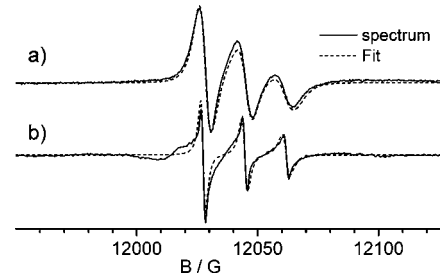

Figure 3. Results of the fit of some experimental EPR spectra of Figure 2: (a) at 230 °C with $\tau_R = 74.1$ ns and $\omega_{ss} = 13.6$ ns; (b) after cooling to 20 °C with $\tau_R = 0.9$ ns; $\omega_{ss} > 1$ ms (after removal of the broad background signal by Fourier filtering).

correlation time τ_R and the time ω_{ss} for the spin exchange between neighboring TEMPO molecules.[33,34] The longer τ_R and the shorter ω_{ss}, the more restricted is the molecular motion of TEMPO and the more anisotropic is the EPR hfs spectrum. However, the EPR excitation frequency has a marked influence on the spectral shape as well, since the ideal isotropic hfs triplet is only seen when the spin exchange frequency and the tumbling rate are fast in comparison to the microwave frequency. When one of the latter two parameters approaches the dimension of the excitation frequency, anisotropic effects are less effectively averaged out and, consequently, the width of the individual hfs lines increases and the whole spectral shape becomes more anisotropic. Thus, for solutions of TEMPOL (that is TEMPO with an OH group in the para position) in *n*-octanol at room temperature, an only weakly anisotropic hfs triplet has been observed in the X-band ($\nu \approx 9.5$ GHz) while spectral anisotropy is more pronounced in the Q-band ($\nu \approx 35$ GHz) (see Supporting Information, Figure S1). The parameters τ_R and ω_{ss} have been derived by spectra simulation using the model of Budil et al.[35] Here we use the same approach to analyze the mobility of TEMPO on the alumina surface (Figure 3).

Satisfactory fits of the strongly anisotropic spectra from 20 to 180 °C (Figure 2), which seem to comprise contributions from TEMPO molecules in rather different surroundings, could not be obtained. However, the more isotropic spectrum of TEMPO/α-Al_2O_3 at 230 °C has been successfully reproduced with $\tau_R = 74.1$ ns and $\omega_{ss} = 13.6$ ns, assuming rotation of the TEMPO molecule about all space directions (Figure 3a). For comparison, TEMPO in a diluted aqueous solution with nonrestricted molecular motion shows values for τ_R of ~0.1 ns.[36] It can be seen from Figure 3 that τ_R is markedly higher for TEMPO molecules supported on the surface of α-Al_2O_3 at 230 °C, suggesting that even at this high temperature effective immobilization hinders the free rotation. Surprisingly, the TEMPO radical is still stable up to 230 °C upon heating in air. A significant change is evident after recooling to 20 °C (Figure

(29) Breysse, M.; Afanasiev, P.; Geantet, C.; Vrinat, M. *Catal. Today* **2003**, *86*, 5–16.
(30) Meille, V. *Appl. Catal., A* **2008**, *348*, 1–15.
(31) Severn, J. R.; Chadwick, J. C.; Duchateau, R.; Friederichs, N. *Chem. Rev.* **2005**, *105*, 4073–4147.
(32) Kishore, M. J. L.; Mishra, G. J.; Kumar, A. *J. Mol. Catal. A: Chem.* **2004**, *216*, 157–163.
(33) Strehmel, V.; Laschewsky, A.; Stoesser, R.; Zehl, A.; Herrmann, W. *J. Phys. Org. Chem.* **2006**, *19*, 318–325.
(34) Stoesser, R.; Herrmann, W.; Zehl, A.; Strehmel, V.; Laschewski, A. *ChemPhysChem* **2006**, *7*, 1106–1111.
(35) Budil, D. E.; Lee, S.; Saxena, S.; Freed, J. H. *J. Magn. Reson. A* **1996**, *120*, 155–189.
(36) Herrmann, W.; Stösser, R.; Moll, K.-P.; Borchert, H.-H. *Appl. Magn. Reson.* **2005**, *28*, 85–106.

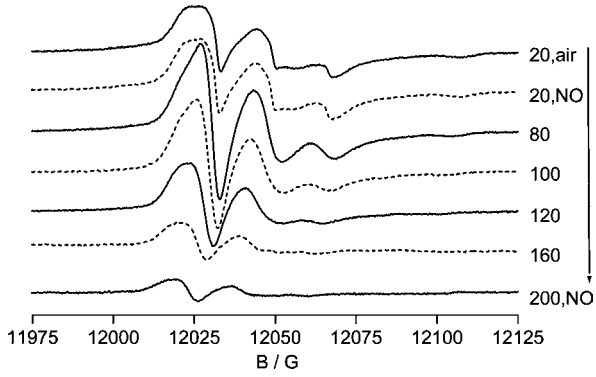

Figure 4. Q-band EPR spectra of TEMPO/α-Al_2O_3 recorded during heating in a flow of 2 vol % NO/N_2. Arrow denotes sequence of treatment.

2). The spectrum now reflects a superposition of two subsignals, a very narrow triplet and a broad background signal. The less anisotropic triplet with narrow lines can be reproduced with a much lower value of $\tau_R = 0.9$ ns and a significantly higher spin exchange time of $\omega_{ss} > 1$ ms (Figure 3b). This suggests that TEMPO molecules moved to less rigidly confined surface positions or into pores of the structure where they can rotate more freely than before. Since these species comprise only a small part of the total number of TEMPO molecules, their mutual distance is larger and the spin exchange between them is less effective than the case before heating.

When TEMPO/α-Al_2O_3 is exposed to a flow of 2 vol % NO/N_2 at 20 °C, almost no change of the signal shape is observed (Figure 4). However, upon heating to 80 °C the width of the TEMPO signal decreases and its amplitude rises markedly in comparison to the respective spectra in air flow (compare Figure 2). The reason might be that TEMPO molecules are displaced by NO from their initial surface positions and, thus, become more mobile. Upon further heating the signal intensity deceases irreversibly while the shape of the spectra becomes similar to that before heating again. This is a clear indication that TEMPO undergoes a chemical reaction with NO. Finally, only those radicals survive which are best protected by the matrix.

Simulation of the EPR spectrum at 60 °C results in values of $\tau_R = 851.6$ ns and $\omega_{ss} = 12.8$ ns, which change to $\tau_R = 656.4$ and 14.5 ns at 80 °C (Figure S2, Supporting Information). In comparison to the EPR spectrum of TEMPO/α-Al_2O_3 at 230 °C under air flow, these values suggest a much stronger restriction of molecular mobility, which may be due first of all to the lower temperature but also to the interaction with NO, which is paramagnetic as well and might contribute to spin exchange. A separate EPR signal of NO adsorbed on Al_2O_3 cannot be discerned in Figure 4. However, it cannot be excluded that this is superimposed on the TEMPO signal, since NO adsorbed on an Al^{3+} Lewis site gives rise to similar hyperfine coupling constants of $A_N \approx 16-32$ G.[37]

When the same experiment is performed with TEMPO supported on pseudoboehmite, AlOOH, a similar behavior like that on α-Al_2O_3 is observed; however, the respective effects take place already at a markedly lower temperature (compare Figures 4 and 5). A pronounced signal narrowing and intensity increase, reflecting the displacement of TEMPO by NO from confined surface positions, are visible already at 20 °C. The much higher mobility of TEMPO under these conditions is also

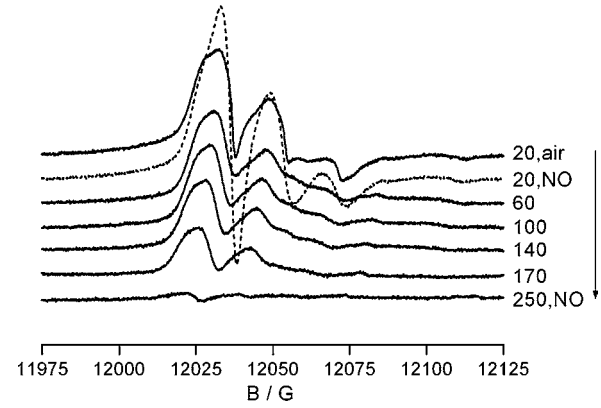

Figure 5. Q-band EPR spectra of TEMPO/AlOOH recorded during heating in a flow of 2 vol % NO/N_2. Arrow denotes sequence of treatment.

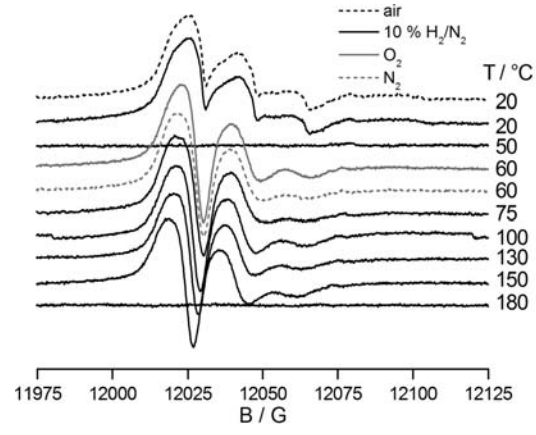

Figure 6. Q-band EPR spectra of TEMPO/AlOOH recorded during heating in various atmospheres. Arrow denotes sequence of treatment.

evident from values of $\tau_R = 30.2$ ns and $\omega_{ss} = 8$ ns, which have been derived from the experimental spectrum at 20 °C in Figure 5 by spectra simulation (Figure S3, Supporting Information). At 60 °C the TEMPO signal starts to decline irreversibly (Figure 5).

These differences in comparison to the TEMPO/α-Al_2O_3 system arise from the fact that, during milling of AlOOH, traces of water are liberated while α-Al_2O_3 particles in the nanometer range are formed. It is well-known that pseudoboehmite releases water and is converted to α-Al_2O_3 upon mechanical and thermal treatments.[38] This could happen, too, during milling, which might cause local heating as well. These water traces might promote the reaction of TEMPO with NO. With rising temperature, a fraction of the TEMPO molecules becomes mobile and may preferentially react with water and NO. This reaction should lead to the corresponding (diamagnetic) hydroxylamine,[39] thus, diminishing the total spectral intensity, while the residual TEMPO molecules remain more strongly immobilized and less accessible to reactants, as reflected by the strong anisotropy of the EPR signal up to 170 °C (Figure 5).

When the TEMPO/AlOOH sample is heated in a flow of 10 vol % H_2/N_2, there is not yet any reaction at 20 °C (Figure 6). At 50 °C the TEMPO radicals disappear upon reduction; however they can be completely reoxidized in an O_2 flow at 60 °C. Then, the sample was flushed in a N_2 flow at 60 °C.

(37) Gutsze, A.; Plato, M.; Karge, H. G.; Witzel, F. *J. Chem. Soc., Faraday Trans.* **1996**, *28*, 2495–2498.

(38) Nofz, M.; Stösser, R.; Scholz, G.; Dörfel, I.; Schultze, D. *J. Eur. Ceram. Soc.* **2005**, *25*, 1095–1107.

(39) Hochkirch, U. PhD Thesis, Humboldt-University of Berlin, 2007.

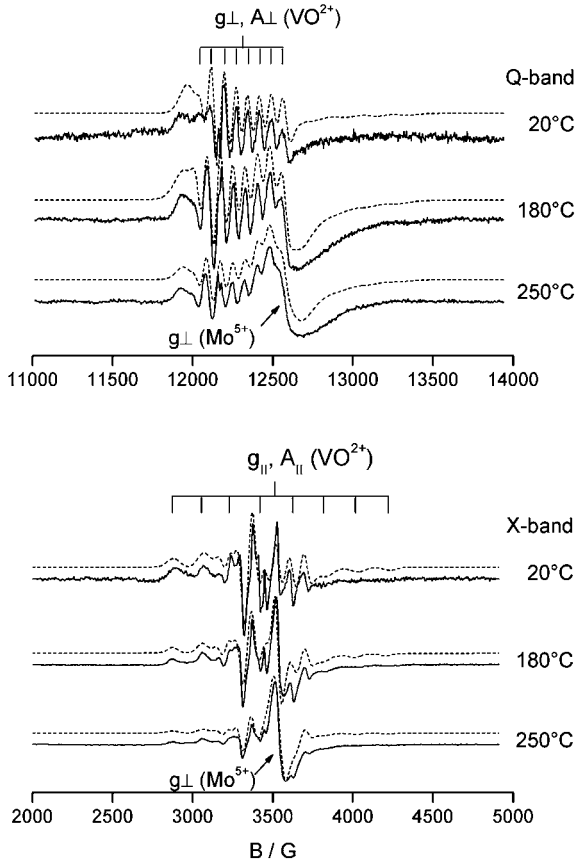

Figure 7. Experimental (solid lines) and calculated (dashed lines) Q-band and X-band EPR spectra of HPVMo during heating in a flow of MeOH/N_2. Spin Hamiltonian parameters derived by spectra simulation are listed in Table 1.

Interestingly, when switching again to 10 vol % H_2/N_2, the EPR signal is now stable up to 150 °C. Obviously, reduction and reoxidation are connected with migration and trapping of the TEMPO radicals in energetically more favorable sites in which they are more stable against H_2.

2.3. Reactions of $H_4PVMo_{11}O_{40}\cdot xH_2O$. Q- and X-band EPR spectra recorded during treatment in 9.8 mol % MeOH/N_2 flow are plotted in Figure 7. At 20 °C, the X-band spectrum shows the characteristic signal of isolated VO^{2+} species with axial symmetry of the *g* and *A* tensor, which consists of two superimposed groups of eight hyperfine structure (hfs) lines, arising from the coupling of the unpaired electron spin ($S = 1/2$) with the nuclear spin of vanadium ($I = 7/2$). Comparison of the experimental spectra in Figure 7 readily shows that hfs lines belonging to the perpendicular components of the *g* and *A* tensor are much better resolved in the Q-band, while they are hard to distinguish in the X-band due to the superposition with the central hfs lines of $g_{||}$ and $A_{||}$. Vice versa, the parallel hfs multiplet is better resolved in the X-band, since the outer lines are not superimposed and particularly very visible at low field.

From the X-band spectra in Figure 7 it is also evident that parallel hfs lines are markedly broader than the perpendicular ones. The reason for this broadening might be a certain distribution of the $g_{||}$ and $A_{||}$ values throughout the vanadyl sites in the sample, which is obviously more pronounced for the parallel rather than the perpendicular components of *g* and *A*. From eq 2 (see Experimental Section) it is evident that the *g* tensor components depend on the magnetic field. Thus, the distribution of $g_{||}$ will lead to stronger line broadening at a higher magnetic field in the Q-band. This is indeed observed in Figure 7. In comparison to the X-band, the parallel hfs lines are no longer well resolved in the Q-band but superimpose to a broad feature hidden by the well resolved perpendicular hfs octet. Therefore it is very difficult to derive reliable values for $g_{||}$ and $A_{||}$ from Q-band spectra while the same is true for $g_\perp$ and $A_\perp$ in the X-band. However, by combined evaluation of Q- and X-band spectra measured under similar conditions both parallel and perpendicular *g* and *A* tensor components can be derived with a precision high enough to serve as starting values for spectra simulation. Thus obtained $g_{||}$, $A_{||}$, $g_\perp$, and $A_\perp$ values have been fitted to the experimental spectra in Figure 7, resulting in the calculated spectra (dashed lines) and the parameters listed in Table 1. It can be seen that, as required, reasonable fits can be obtained in both frequency bands with the same set of *g* and *A* parameters but a different line width.

Table 1. Spin Hamiltonian Parameters Derived by Simulation of HPVMo EPR Spectra

band	species	$g_{||}$, $g_\perp$	$\lvert A_{||}\rvert$, $\lvert A_\perp\rvert$ [G]	$\Delta B_{||}$, $\Delta B_\perp$ [G]	I_{rel} [%][a]	β_2^{*2} $\Delta g_{||}/\Delta g_\perp$
		spectra at 20 °C in MeOH/N_2 flow				
Q	V^{4+}	1.924, 1.978	194, 72	120, 46	93.7	
	Mo^{5+}	1.934, 1.941	–	884, 37	6.3	0.85
X	V^{4+}	1.924, 1.978	194, 72	81, 49	92.6	3.22
	Mo^{5+}	1.934, 1.941	–	823, 33	7.4	
		spectra at 180 °C in MeOH/N_2 flow				
Q	V^{4+}	1.932, 1.981	194, 72	132, 49	47.4	
	Mo^{5+}	1.935, 1.939	–	832, 154	52.6	0.84
X	V^{4+}	1.932, 1.981	194, 72	63, 47	47.5	3.30
	Mo^{5+}	1.935, 1.939	–	938, 33	52.5	
		spectra at 250 °C in MeOH/N_2 flow				
Q	V^{4+}	1.930, 1.981	192, 75	111, 48	26.4	
	Mo^{5+}	1.909, 1.940	–	832, 154	73.6	0.81
X	V^{4+}	1.930, 1.981	192, 75	77, 46	58.1	3.40
	Mo^{5+}	1.909, 1.940	–	101, 73	41.9	
		spectra at 250 °C in MeOH/air flow				
Q	V^{4+}	1.925, 1.981	194, 75	126, 50	90.0	
	Mo^{5+}	1.934, 1.941	–	817, 39	10.0	0.83
X	V^{4+}	1.925, 1.981	194, 75	82, 50	84.4	3.63
	Mo^{5+}	1.934, 1.941	–	857, 32	15.6	
		spectra at 230 °C in HCHO/N_2 flow				
Q	V^{4+}	1.928, 1.981	193, 75	90, 29	15.8	
	Mo^{5+}	1.935, 1.938	–	865, 128	84.2	0.82
X	V^{4+}	1.928, 1.981	193, 75	38, 28	68.2	3.50
	Mo^{5+}	1.935, 1.938	–	830, 31	31.8	
		spectra at 230 °C in HCHO/air flow				
Q	V^{4+}	1.931, 1.982	192, 74	137, 55	99.0	
	Mo^{5+}	1.934, 1.941	–	882, 38	1.0	0.82
X	V^{4+}	1.931, 1.982	192, 74	89, 51	96.7	3.51
	Mo^{5+}	1.934, 1.941	–	831, 44	3.3	

With rising temperature, not only V^{5+} but also Mo^{6+} is reduced in the MeOH/N_2 flow giving rise to an additional signal with axial *g* tensor symmetry but without observable hfs caused by Mo^{5+} (Table 1, Figure 7). This line is superimposed on the middle field part of the V^{4+} hfs signal in the X-band, where it is nearly indistinguishable from the latter but appears on the high field tail of the Q-band spectrum where it is much better separated from the perpendicular V^{4+} hfs lines. Consequently, a better agreement between the experimental and calculated spectrum could be obtained in the Q-band at 250 °C in the MeOH/N_2 flow (Figure 7). In particular, the percentage to which the Mo^{5+} signal contributes to the overall spectral intensity is more reliable from the Q-band simulation.

When the same experiment is performed in a flow of 9.8 mol % MeOH/air, the intensity of the VO^{2+} signal follows more or less the same behavior as that in MeOH/N_2; however, the Mo^{5+} line is markedly suppressed (Figure 8). A direct comparison of

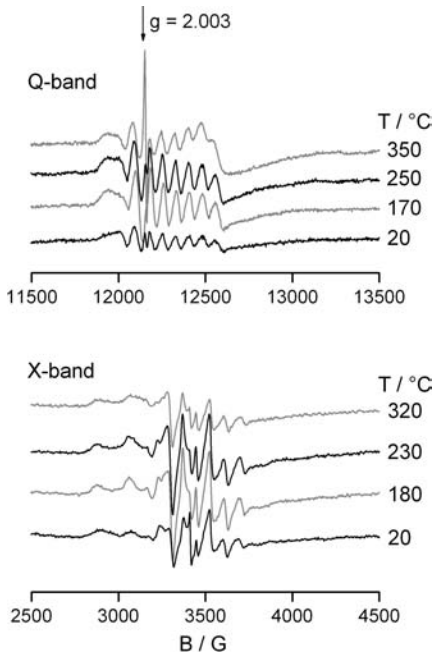

Figure 8. Q-band and X-band EPR spectra of HPVMo during heating in a flow of MeOH/air.

the intensities of the respective spectra in MeOH/N_2 and MeOH/air is available from Figure S4 in the Supporting Information). This indicates that reduction of Mo^{6+} to Mo^{5+} is less probable than the reduction of V^{5+} to V^{4+} and/or reoxidation of Mo^{5+} is faster than reoxidation of V^{4+} in the presence of air. Moreover, a very narrow line arises with increasing temperature in the MeOH/air flow in the Q-band spectrum (Figure 8, marked by arrow). This line is most probably due to carbon radicals, being present in carbon deposits which might be formed on the surface by dehydrogenation of methanol. This signal cannot be identified in the X-band, due to superposition with the VO^{2+} hfs signal. Interestingly, the carbon radical signal is well pronounced in the Q-band spectra in the MeOH/air flow but hardly seen in the MeOH/N_2 flow (Figure 8). However, without oxygen in the feed, carbon deposits should be formed to a higher amount than in the presence of air.

The higher intensity of the radical signal in the MeOH/air flow may be due to the fact that in the presence of air only weakly aggregated carbon species are formed. In such species, antiferromagnetic interactions between neighboring radicals might not be as dominating as in the highly polymeric coke species which are probably formed in the absence of air. Obviously, this renders the radical signals visible in the Q-band.

Molybdate catalysts, in particular iron molybdates,[40] are used for the industrial production of formaldehyde (FA) by selective oxidation of methanol. Since FA may also be formed upon contact of HPVMo with methanol, the interaction of FA with HPVMo in the presence of N_2 and air, respectively, has also been studied in both frequency bands using a flow containing 1.8 mol % FA and 5.0 mol % H_2O in either nitrogen or air (Figure 9). The percentage of FA in this feed would be similar to a hypothetic FA selectivity of 20% in the product stream when a feed stream with 9.8% MeOH is used. In the absence of oxygen, a signal due to Mo^{5+} is visible above 180 °C, which becomes more pronounced with rising temperature up to 320

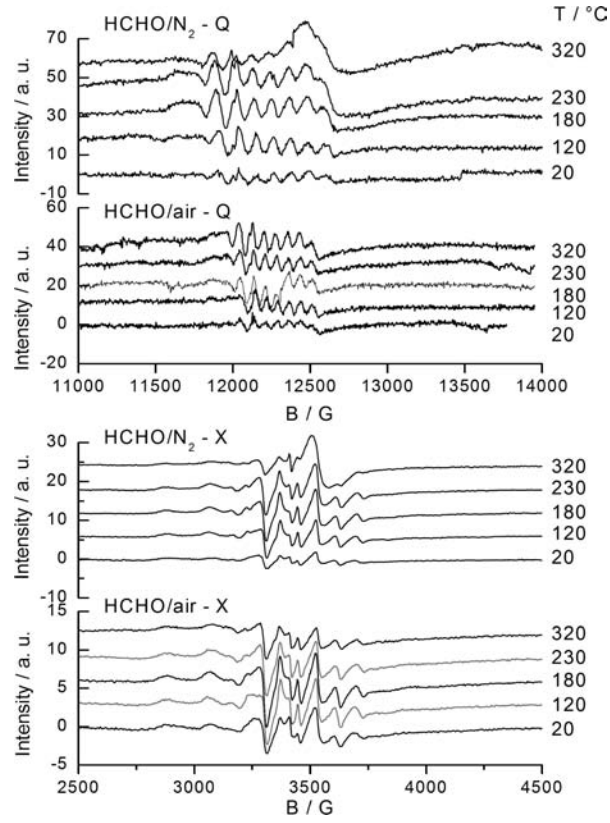

Figure 9. Q-band and X-band EPR spectra of HPVMo during heating in a flow of MeOH/N_2 and MeOH/air.

°C. In contrast, reduction of Mo^{6+} to Mo^{5+} is negligible in the FA/H_2O/air flow (Figure 9). In general, this behavior is similar to the one observed in MeOH/N_2 and MeOH/air flows, although the extent of reduction is less pronounced in the presence of FA. However, in the latter case the percentage of hydrocarbon in the feed was by a factor of ~5 smaller. To explore the reduction behavior under comparable conditions of hydrocarbon concentration, an experiment with the same flow rate but a feed containing 1.8 mol % MeOH and 5.0 mol % water in nitrogen or air was also performed, however only in X-band. A comparison of the X-band spectra of this experiment with the X-band spectra in Figure 9 is shown in Figure S5 (see Supporting Information). The signal intensities are very similar in both experiments, suggesting that the reductive properties of MeOH and FA do not differ much. This holds accordingly also for the air-containing feed however; in this case reduction of Mo^{6+} to Mo^{5+} is widely suppressed.

More detailed information on structural changes of the V^{4+} sites can be obtained from the parameters $\Delta g_{\|}/\Delta g_{\perp}$ and $\beta_2{}^{*2}$. $\Delta g_{\|}/\Delta g_{\perp}$ (with $\Delta g_{\|} = g_{\|} - g_e$ and $\Delta g_{\perp} = g_{\perp} - g_e$) is a measure for the total axial distortion. The higher $\Delta g_{\|}/\Delta g_{\perp}$, the shorter is the V═O and the longer are the bonds in the equatorial plane of the VO^{2+} site.[41] The so-called in-plane delocalization coefficient $\beta_2{}^{*2}$ (obtained by eq 1 with $P = 184.5$ G[42]) reflects the extent to which the free electron is delocalized toward the ligands in the basal plane of the VO^{2+} species. $\beta_2{}^{*2} = 1$ for a pure VO^{2+} ion and decreases with rising covalent character of the bonds in the basal plane.

(40) Vieira Soares, A. P.; Farinha Portela, M.; Kiennemann, A. *Catal. Rev. Sci. Eng.* **2005**, *47*, 125–174.

(41) Novinska, K.; Wieckowski, A. B. *Z. Phys. Chem. N. F.* **1989**, *162*, 231–244.

(42) Boucher, L. J.; Tynan, E. C.; Yen, T. F. *Electron Spin Resonance of Metal Complexes*; Plenum Press: New York, 1969; p 111.

$$\beta_2{}^{*2} = 7/6\Delta g_{||} - 5/12\Delta g_{\perp} - 7/6[(A_{||} - A_{\perp})/P] \qquad (1)$$

From Table 1 it can be seen that $\Delta g_{||}/\Delta g_{\perp}$ increases with rising temperature in the presence of MeOH, while $\beta_2{}^{*2}$ decreases. This might be an indication that the hydrocarbon starts to react with the VO^{2+} sites, possibly by interaction of its OH group with an oxygen from the equatorial plane of the $O_4V{=}O$ site (Scheme 2).

It is probable that the unpaired electron of the V^{4+} site is more delocalized toward the equatorial oxygen ligands forming the hydrogen bridge, which is reflected by the decreasing $\beta_2{}^{*2}$ values. On the other hand, this may distort the $O_4V{=}O$ even more, as can be seen from the increasing $\Delta g_{||}/\Delta g_{\perp}$ values. Interestingly, these effects are almost the same when HCHO is used as a reactant, suggesting that a similar C−H·····O−V interaction can occur. Obviously, this interaction is not much influenced by the presence of oxygen in the feed since the $\Delta g_{||}/\Delta g_{\perp}$ and $\beta_2{}^{*2}$ values do not change markedly under these conditions (Table 1).

3. Conclusions

A novel setup for recording in situ EPR spectra of solid catalysts under reaction conditions at elevated temperatures in the Q-band ($\nu \approx 35$ GHz) has been developed for the first time. It has been shown that the application potential of in situ EPR spectroscopy for monitoring heterogeneous catalytic reactions can be markedly widened by recording EPR spectra at a higher microwave frequency. Additional benefits may be anticipated when the experimental technique is further improved by coupling with online product analysis as well as by using advanced simulation procedures (e.g., the application of models involving statistical distributions of dynamic parameters for paramagnetic species in different states of immobilization or different states of chemical reactivity). In combination with results from common X-band EPR studies, new insights in the progress of catalytic reactions can be gained, due to the wider accessible range of microwave frequency, magnetic field, and time.

Thus, Q-band EPR spectra of TEMPO radicals adsorbed on two different aluminum oxide and hydroxide supports have been recorded up to 230 °C in different gas flows and successfully fitted by a dynamic model, which delivered semiquantitative information on their mobility on the support surface as well as on their interaction with reactants such as NO, H_2O, H_2, and O_2.

Particular benefits result from the combined evaluation of in situ X-band and in situ Q-band spectra recorded from a supported $H_4PVMo_{11}O_{40}$ catalyst during contact with methanol and formaldehyde. While X-band spectra provide high resolution for the parallel g and A tensor components of the VO^{2+} sites, this is true for the perpendicular g and A tensor components of VO^{2+} as well as for Mo^{5+} sites in the Q-band. Thus, combining measurements in the two frequency bands can help to interpret complex spectra with superimposed signals from several paramagnetic species, which frequently do exist in real transition metal oxide catalysts.

4. Experimental Section

4.1. In Situ EPR Measurements. EPR spectra in the Q-band were recorded on an ELEXSYS 500-10/12 cw spectrometer equipped with an ER051QG microwave bridge (Bruker) and connected to a homemade cylindrical cavity (Figure 10). Construction details of this cavity are provided in the Supporting Information (Figure S6). A quartz capillary plug-flow reactor with 2 mm outer diameter, containing ~2 mg of the solid sample (corresponding to 5 mm bed height), and surrounded by a quartz dewar mantle was directly placed inside this cavity and connected to a gas-dosing device equipped with mass flow controllers (Figure 10). The reactor was heated up to 350 °C by a preheated stream of nitrogen. The cavity was cooled from the outside by a flow of compressed air. In situ EPR measurements in X-band were recorded on the same spectrometer in a commercial rectangular X-band cavity (Bruker), in which a previously described double-wall quartz dewar was implemented. To ensure the same flow conditions as those in the Q-band experiments, the Q-band reactor tube was also implemented in the X-band cavity, connected to the same gas dosing device, and heated by a commercial temperature control unit using a preheated stream of nitrogen.[43] Spectra were recorded with a modulation frequency of 100 kHz, a microwave power of 6.3 mW, and a modulation amplitude of 5 G. The reactant feed was mixed by bubbling a flow of N_2 or air (15 mL/min) through a saturator filled with MeOH or EtOH, respectively, to result in alcohol contents of 9.8 mol %. Alternatively, the same experiments were performed with solutions of 26 mol % of formaldehyde or methanol in water, resulting in feed compositions of 1.8 mol % formaldehyde or methanol, respectively, and 5.0 mol % water vapor in nitrogen or air.

Scheme 2. Possible Interaction of MeOH with a VO^{2+} Site

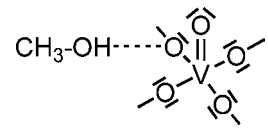

4.2. EPR Spectra Calculation. EPR spectra of supported TEMPO molecules have been calculated with the model of Budil et al.[35] EPR spectra of $H_4PVMo_{11}O_{40}{\cdot}xH_2O$ were calculated with the program SIM14S of Lozos et al.[44] using eq 2 for the spin Hamiltonian

$$H = \mu_B \cdot S \cdot g \cdot B_0 + SAI \qquad (2)$$

in which μ_B is the Bohr magneton, S is the electron spin operator, g is the g tensor, B_0 is the magnetic field vector, A is the hyperfine tensor, and I is the nuclear spin operator.

4.3. Materials. The preparation of the TPO-AlO_x samples (α-Al_2O_3 and AlOOH) has been done by comilling TEMPO (0.01 wt

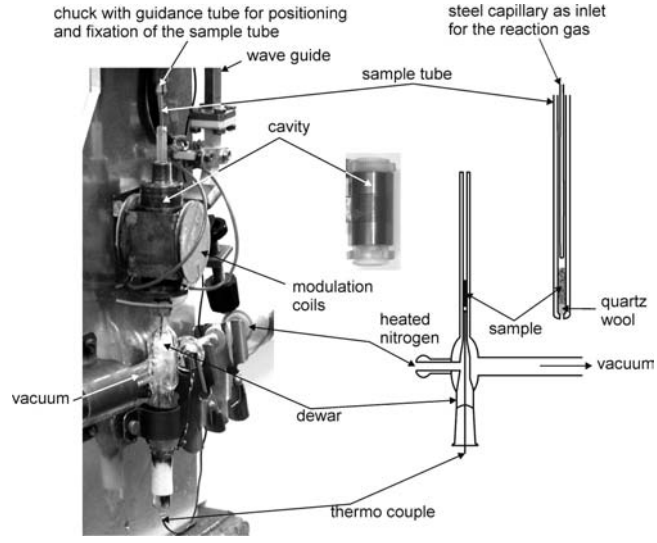

Figure 10. Constituents and arrangement of equipment for Q-band in situ measurements.

%) with the respective matrix for 0.5 h at 600 rpm and 5 balls in a silicon carbide beaker (Pulverisette, Fritsch GmbH, Idar-Oberstein, Germany). $H_4PVMo_{11}O_{40} \cdot x\ H_2O$ was prepared from MoO_3, V_2O_5, and 85% phosphoric acid as described elsewhere.[23,45] The supported catalyst with an HPVMo loading of 20 wt % was prepared using a commercial silica−alumina support (Siralox 20, Sasol). The support was suspended in an aqueous solution of the acid and stirred at room temperature for 20 h. After water removal in a rotavap at 60 °C, the samples were dried for 2 h at 120 °C and finally heated with 5 K/min in flowing air to 350 °C and calcined for 4 h. Prior to the EPR measurements, the sample was heated again within the reactor to 340 °C and cooled to 20 °C in a N_2 flow to remove adsorbed moisture.

(43) Brückner, A. *Chem. Commun.* **2005**, 1761–1763.
(44) Lozos, G. P.; Hofman, B. M.; Franz, C. G. *Quantum Chemistry Programs Exchange*, 1973, No. 265.
(45) Bardin, B. B.; Davis, R. J. *Appl. Catal., A* **1999**, *185*, 283–292.

Acknowledgment. The authors acknowledge the very valuable contributions of B. Lück and S. Zillmann (Mechanical workshop of the chemical institute of HU Berlin) for manufacturing the Q-band resonator and F. Leinung (Glassblowing workshop, HU Berlin) for producing the Q-band quartz Dewar.

Supporting Information Available: Room temperature EPR spectra of TEMPOL in *n*-octanol measured in the X- and Q-band. Simulation results for selected EPR spectra from Figures 4 and 5. Intensity comparison of EPR spectra of HPVMo during heating in $MeOH/N_2$ and MeOH/air flow. In situ X-band EPR spectra recorded during heating in flows of 5.0 mol % H_2O/N_2 containing 1.8 mol % MeOH or HCHO. Construction details of the Q-band cavity including the reactor. This material is available free of charge via the Internet at http://pubs.acs.org.

JA1035418